ground liver ($P < .05$ with the multiple comparison test). In addition, type B and C nodules had higher densities of arteries and portal veins than did type A nodules ($P < .05$ with the multiple comparison test). In contrast, the density of hepatic veins around type B and C nodules was decreased compared with type A nodules ($P < .05$ with unpaired t test). No significant difference was observed in the density of any perinodular vessels between type B and type C nodules ($P < .05$).

Continuity of vessels at nodule border.—In the type A nodule, which was a DN, serial pathologic slices revealed the continuity between intranodular preexisting hepatic veins and extranodular hepatic veins (Fig 6a, 6b). In addition, intranodular capillarized sinusoids continued into extranodular hepatic veins (Fig 6c, 6d).

We also examined the serial pathologic slices of a type B nodule, which was a moderately differentiated HCC without a fibrous capsule that had a replacing growth pattern, for continuity of intranodular capillarized sinusoids and surrounding hepatic sinusoids (Fig 7). Intranodular and perinodular hepatic veins were rarely observed; therefore, their continuity was not confirmed.

We used two type C moderately differentiated HCCs to examine the continuity of vessels at the tumor border. One demonstrated compressing growth without a fibrous capsule, and the other showed compressing growth with a fibrous capsule. We observed many portal venules within the intranodular fibrous septa and the fibrous capsule, accompanied by hepatic arteries and bile ducts. In the nodule without a fibrous capsule, intranodular capillarized sinusoids connected to extranodular portal veins directly (Fig 8a, 8b). In addition, intranodular capillarized sinusoids connected to portal venules within the fibrous septum, and these portal venules continued into extranodular portal veins (Fig 8c, 8d). In the nodule with a fibrous capsule, intranodular capillarized sinusoids connected to portal venules within the fibrous capsule, with these venules connecting to extranodular portal veins (Fig 9).

Discussion

The different radiologic appearances of type A, B, and C nodules seem to be the direct result of several histologic features: the grade of tumor differentiation, fibrous capsule formation, and tumor growth pattern. According to the theory of multistep hepatocarcinogenesis, we think that these histologic features change as the nodules progress from type A (DN or well-differentiated HCC) to type B to type C (both moderately differentiated HCC). The results of our study suggest that the main drainage vessels change from hepatic veins (type A) to hepatic sinusoids (type B) and then to portal veins (type C) during this progression.

On the basis of our findings, a mechanism for how the drainage vessels of HCC change during multistep hepatocarcinogenesis can be postulated (Fig 10). As the tumor cells become more atypical and proliferate more rapidly, they first invade the intranodular hepatic veins because they are not accompanied by fibrous tissue (eg, Glisson's sheath surrounding portal veins). In the perinodular area, hepatic veins are similarly collapsed by tumor compression. Therefore, intranodular and perinodular hepatic veins disappear earlier than do portal veins. When the drainage through hepatic veins is blocked, drainage flows mainly into surrounding hepatic sinusoids and partially into portal veins according to the blood pressure gradient. As the intranodular cellular density increases, the tumor growth pattern changes from replacing growth to compressing growth, and a thick fibrous capsule is formed by the compressed perinodular liver tissue (25). At this stage, perinodular hepatic sinusoids are collapsed, and the conti-

Figure 10

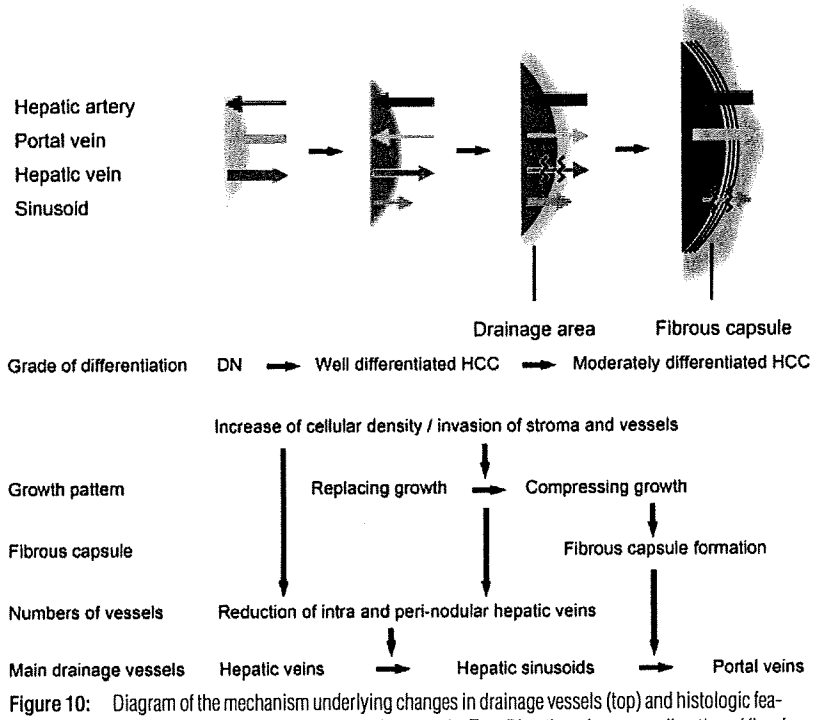

Figure 10: Diagram of the mechanism underlying changes in drainage vessels (top) and histologic features (bottom) of HCC during multistep hepatocarcinogenesis. Top: Direction of arrow = direction of flow for that vessel type. Thickness of arrow = volume through that vessel. Wavy lines through arrow = disruption of flow. Gray area = nodule.

nuity of intranodular and extranodular sinusoids is interrupted by fibrous capsule formation. Therefore, drainage blood flow has no outlet other than through portal veins, accompanied by a marked increase in arterial blood supply. Although the total number of intranodular portal veins is decreased, portal venules are relatively well preserved in the fibrous septa and capsule. These patent portal venules could become the drainage vessels of an established encapsulated HCC.

The direction of hepatic arterial flow is afferent, while that of hepatic venous flow is efferent owing to the pressure gradient. In contrast, the direction of portal flow to nodules is variable and can be determined by using the combination of CTAP and histologic findings. Type C nodules showed no portal perfusion at CTAP, and direct connections between intranodular capillarized sinusoids and portal venules were confirmed with histologic findings. We believe that the direction of portal flow would be efferent in type C nodules. That is, blood flow in portal veins seems to dramatically change during multistep hepatocarcinogenesis from afferent flow in type A nodules to efferent flow in type C nodules.

Previously, perinodular contrast enhancement was thought to represent the presence of a fibrous capsule (26,27). However, as shown in type C nodules, corona enhancement was frequently broader than the histologically confirmed fibrous capsule and included a protruding portion. Moreover, corona enhancement was also seen in nonencapsulated type B and C HCC nodules. Therefore, we conclude that corona enhancement consists of staining of mainly the perinodular parenchyma, although it might contain staining of the fibrous capsule, as well. However, the drainage area of type B nodules was thinner and smoother than that of type C nodules. This difference might be explained by the fact that the draining blood pressure or speed through surrounding hepatic sinusoids (type B nodules) might be lower than that through portal veins (type C nodules). Drainage area of type A nodules could not be observed because contrast material drained directly into the hepatic vein and did not pass through perinodular hepatic sinusoids. The corona enhancement findings at late-phase CTHA are surmised to closely correlate with the histologic changes of drainage vessels.

As has been previously reported (11–17), pathologic changes of arteries and portal veins in DNs and HCC are closely correlated with the radiologic findings. We should keep in mind that the background liver previous studies and ours used as the control does not represent normal liver (mainly chronic liver disease). In comparison to background liver, type A nodules had decreased intranodular arteries, and types B and C had significantly increased intranodular arteries and capillarized sinusoids. The findings on early-phase CTHA images reflected the histologic findings. In contrast, the density of intranodular portal veins decreased from type A to type B and C nodules, which corresponds to the findings on CTAP images.

In addition, we found an interesting pathologic feature; similar to intranodular portal veins, the density of intranodular hepatic veins markedly decreased from type A to type B and C nodules. Density of perinodular hepatic veins was also decreased in type B and C nodules, probably owing to tumor compression, whereas the densities of perinodular portal veins and hepatic arteries were increased. As mentioned above, hepatic veins might more readily collapse than would portal veins because of the absence of perivascular connective tissue. This impairment of blood flow through the hepatic veins could possibly trigger the dramatic change of drainage blood flow into the portal veins.

On the basis of the radiologic findings of our study, particularly corona enhancement, imaging can be used to provide insight into the grade of malignancy or drainage vessels of hepatocellular nodules. Drainage vessels seem to be a main factor in determining tumor progression, therefore understanding the drainage routes of HCC has implications for interventional therapy (eg, transarterial chemoembolization or ablation) and surgical resection (18,28). At transarterial chemoembolization of hypervascular HCCs, outflow of iodized oil into perinodular portal veins or surrounding parenchyma is often observed (29,30). This finding suggests that the drainage vessels are portal veins or sinusoids. Nodule drainage has been shown to influence the treatment efficacy of transarterial chemoembolization (31).

Our study had several limitations. First, serial slices of only four nodules were used to evaluate the continuity of vessels at the nodule border. In the remaining nodules the drainage route was surmised from the number of vessels in the tumor and surrounding liver in correlation with the CTAP and CTHA findings. Second, quantitative analysis of all drainage vessels was not feasible. Therefore, in the case of mixed drainage routes (eg, portal veins and surrounding hepatic sinusoids), the main route could not be accurately determined. However, we do not believe these factors negate the new concept proposed in our study.

In conclusion, the main drainage vessels of hepatocellular nodules change from hepatic veins to surrounding hepatic sinusoids and then to portal veins during multistep hepatocarcinogenesis. This change seems to be triggered by the early disappearance of intranodular and perinodular hepatic veins. This notion is important for understanding pathophysiologic and radiologic features of DN, early HCC, and moderately differentiated HCC.

References

1. Villa E, Baldini GM, Pasquinelli C, et al. Risk factors for hepatocellular carcinoma in Italy: male sex, hepatitis B virus, non-A non-B infection, and alcohol. Cancer 1988;62:611–615.

2. Unoura M, Kaneko S, Matsushita E, et al. High-risk groups and screening strategies for early detection of hepatocellular carcinoma in patients with chronic liver disease. Hepatogastroenterology 1993;40:305–310.

3. Takayama T, Makuuchi M, Hirohashi S, et al. Malignant transformation of adenomatous hyperplasia to hepatocellular carcinoma. Lancet 1990;336:1150–1153.

4. Sakamoto M, Hirohashi S, Shimosato Y. Early stages of multistep hepatocarcinogenesis: adenomatous hyperplasia and early hepatocellular carcinoma. Hum Pathol 1991;22:172–178.
5. Kobayashi M, Ikeda K, Hosaka T, et al. Dysplastic nodules frequently develop into hepatocellular carcinoma in patients with chronic viral hepatitis and cirrhosis. Cancer 2006; 106:636–647.
6. Nakanuma Y, Terada T, Terasaki S, et al. Atypical adenomatous hyperplasia in liver cirrhosis: low-grade hepatocellular carcinoma or borderline lesion? Histopathology 1990;17:27–35.
7. Nakanuma Y, Terada T, Ueda K, Terasaki S, Nonomura A, Matsui O. Adenomatous hyperplasia of the liver as a precancerous lesion. Liver 1993;13:1–9.
8. Terminology of nodular hepatocellular lesions: International Working Party. Hepatology 1995;22:983–993.
9. Nakashima O, Sugihara S, Kage M, Kojiro M. Pathomorphologic characteristics of small hepatocellular carcinoma: a special reference to small hepatocellular carcinoma with indistinct margins. Hepatology 1995; 22:101–105.
10. Nakano M, Saito A, Yamamoto M, Doi M, Takasaki K. Stromal and blood vessel wall invasion in well-differentiated hepatocellular carcinoma. Liver 1997;17:41–46.
11. Matsui O, Kadoya M, Kameyama T, et al. Benign and malignant nodules in cirrhotic livers: distinction based on blood supply. Radiology 1991;178:493–497.
12. Hayashi M, Matsui O, Ueda K, Kawamori Y, Gabata T, Kadoya M. Progression to hypervascular hepatocellular carcinoma: correlation with intranodular blood supply evaluated with CT during intraarterial injection of contrast material. Radiology 2002;225:143–149.
13. Matsui O, Takashima T, Kadoya M, et al. Dynamic computed tomography during arterial portography: the most sensitive examination for small hepatocellular carcinomas. J Comput Assist Tomogr 1985;9:19–24.
14. Takayasu K, Muramatsu Y, Furukawa H, et al. Early hepatocellular carcinoma: appearance at CT during arterial portography and CT arteriography with pathologic correlation. Radiology 1995;194:101–105.
15. Murakami T, Takamura M, Kim T, et al. Double phase CT during hepatic arteriography for diagnosis of hepatocellular carcinoma. Eur J Radiol 2005;54:246–252.
16. Tajima T, Honda H, Taguchi K, et al. Sequential hemodynamic change in hepatocellular carcinoma and dysplastic nodules: CT angiography and pathologic correlation. AJR Am J Roentgenol 2002;178:885–897.
17. Hayashi M, Matsui O, Ueda K, et al. Correlation between the blood supply and grade of malignancy of hepatocellular nodules associated with liver cirrhosis: evaluation by CT during intraarterial injection of contrast medium. AJR Am J Roentgenol 1999;172:969–976.
18. Park YN, Yang CP, Fernandez GJ, Cubukcu O, Thung SN, Theise ND. Neoangiogenesis and sinusoidal "capillarization" in dysplastic nodules of the liver. Am J Surg Pathol 1998; 22:656–662.
19. Ueda K, Terada T, Nakanuma Y, Matsui O. Vascular supply in adenomatous hyperplasia of the liver and hepatocellular carcinoma: a morphometric study. Hum Pathol 1992;23: 619–626.
20. Toyosaka A, Okamoto E, Mitsunobu M, Oriyama T, Nakao N, Miura K. Intrahepatic metastases in hepatocellular carcinoma: evidence for spread via the portal vein as an efferent vessel. Am J Gastroenterol 1996;91: 1610–1615.
21. Tochio H, Kudo M. Afferent and efferent vessels of premalignant and overt hepatocellular carcinoma: observation by color Doppler imaging. Intervirology 2004;47:144–153.
22. Ueda K, Matsui O, Kawamori Y, et al. Hypervascular hepatocellular carcinoma: evaluation of hemodynamics with dynamic CT during hepatic arteriography. Radiology 1998;206:161–166.
23. Hirohashi S, Ishak KG, Kojiro M, et al. Hepatocellular carcinoma. In: Hamilton SR, Aaltonen LA, eds. Pathology and genetics of tumours of the digestive system. Lyon, France: IARC, 2000; 157–172.
24. Nakamura K, Zen Y, Sato Y, et al. Vascular endothelial growth factor, its receptor Flk-1, and hypoxia inducible factor-1alpha are involved in malignant transformation in dysplastic nodules of the liver. Hum Pathol 2007;38:1532–1546.
25. Okuda K, Musha H, Nakajima Y, et al. Clinicopathologic features of encapsulated hepatocellular carcinoma: a study of 26 cases. Cancer 1977;40:1240–1245.
26. Ros PR, Murphy BJ, Buck JL, Olmedilla G, Goodman Z. Encapsulated hepatocellular carcinoma: radiologic findings and pathologic correlation. Gastrointest Radiol 1990; 15:233–237.
27. Lim JH, Choi D, Park CK, Lee WJ, Lim HK. Encapsulated hepatocellular carcinoma: CT-pathologic correlations. Eur Radiol 2006;16: 2326–2333.
28. Sakon M, Nagano H, Nakamori S, et al. Intrahepatic recurrence of hepatocellular carcinoma after hepatectomy. Arch Surg 2002; 137:94–99.
29. Matsui O, Kadoya M, Yoshikawa J, et al. Small hepatocellular carcinoma: treatment with subsegmental transcatheter arterial embolization. Radiology 1993;188:79–83.
30. Terayama N, Matsui O, Gabata T, et al. Accumulation of iodized oil within the nonneoplastic liver adjacent to hepatocellular carcinoma via the drainage routes of the tumor after transcatheter arterial embolization. Cardiovasc Intervent Radiol 2001;24:383–387.
31. Miyayama S, Matsui O, Yamashiro M, et al. Ultraselective transcatheter arterial chemoembolization with a 2-f tip microcatheter for small hepatocellular carcinomas: relationship between local tumor recurrence and visualization of the portal vein with iodized oil. J Vasc Interv Radiol 2007;18:365–376.

Journal of Medical Imaging and Radiation Oncology **53** (2009) 271–282

PICTORIAL ESSAY

Anastomosis between the hepatic artery and the extrahepatic collateral or between extrahepatic collaterals: Observation on angiography

S Miyayama,[1] M Yamashiro,[1] M Okuda,[1] H Aburano,[1] N Shigenari,[1] K Morinaga[1] and O Matsui[2]

[1]Department of Diagnostic Radiology, Fukuiken Saiseikai Hospital, Fukui, and [2]Department of Radiology, Kanazawa University Graduate School of Medical Science, Kanazawa, Japan

S Miyayama MD; **M Yamashiro** MD; **M Okuda** MD; **H Aburano** MD; **N Shigenari** MD; **K Morinaga** MD; **O Matsui** MD

Correspondence
Dr Shiro Miyayama, Department of Diagnostic Radiology, Fukuiken Saiseikai Hospital, 7-1, Funabashi, Wadanaka-cho, Fukui 918-8503, Japan.
Email: s-miyayama@fukui.saiseikai.or.jp

Conflicts of interest: None.

Submitted 19 July 2008; accepted 27 August 2008.

doi:10.1111/j.1440-1673.2009.02073.x

Summary

Transcatheter arterial chemoembolisation for hepatocellular carcinoma is widely carried out not only through the hepatic artery but also through the extrahepatic collateral pathways. Anatomically, there are many anastomoses between the hepatic artery and the extrahepatic collateral as well as among the extrahepatic collaterals. However, these anastomoses may not be shown on angiography because the anastomosing braches are too small. These anastomoses may not only interfere with effective control of hepatocellular carcinoma by transcatheter arterial chemoembolisation but also cause unexpected procedure-related complications. Therefore, radiologists should have sufficient knowledge of these underlying anastomoses. In this report, we present our angiographic images.

Key words: anastomosis; extrahepatic collateral pathway; hepatocellular carcinoma; transcatheter arterial chemoembolisation.

Introduction

Hepatocellular carcinoma is frequently supplied by an extrahepatic collateral pathway.[1–11] Transcatheter arterial chemoembolisation (TACE) via the hepatic artery and extrahepatic collaterals is widely accepted to manage unresectable tumours.[1–11]

The hepatic arterial system and extrahepatic collaterals or two or more different extrahepatic collaterals anastomose with each other.[12] Anatomically, anastomoses between the hepatic artery and the extrahepatic collateral or between extrahepatic collaterals are well known; however, there are only a few reports of these imaging findings.[7,10] Anastomoses between these vessels may cause not only incomplete therapeutic effects of TACE but also unexpected procedure-related complications; therefore, it is very important to become thoroughly familiar with such anastomoses.

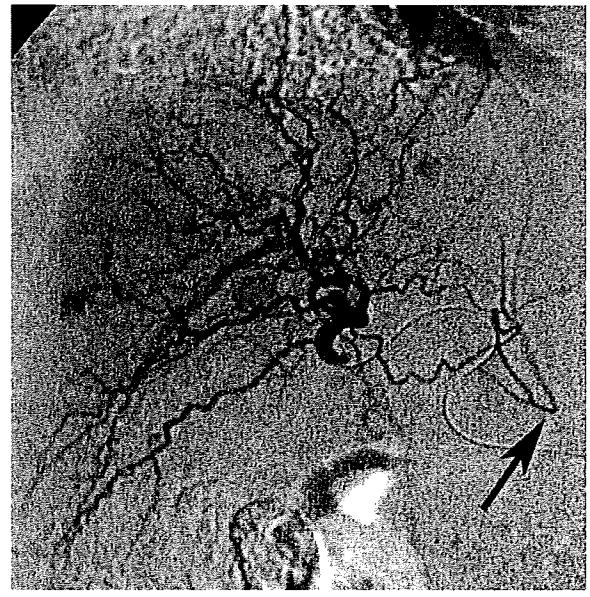

Fig. 1. Arteriogram of the right hepatic artery shows multiple tumour stains and anastomosis between the caudate arterial branch of the liver and the right inferior phrenic artery (arrow).

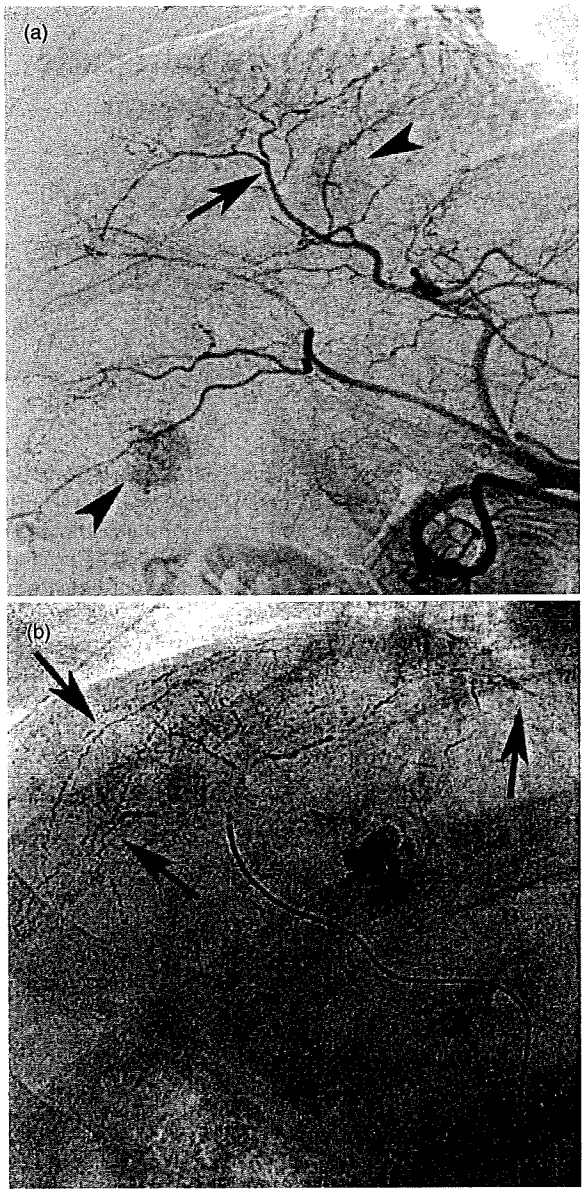

Fig. 2. (a) Coeliac arteriogram shows multiple tumour stains in the liver (arrowheads). First, a small branch of the medial segmental artery was selected (arrow), and transcatheter arterial chemoembolisation was carried out. (b) Spot radiograph during chemoembolisation shows branches of the right inferior phrenic artery (arrows).

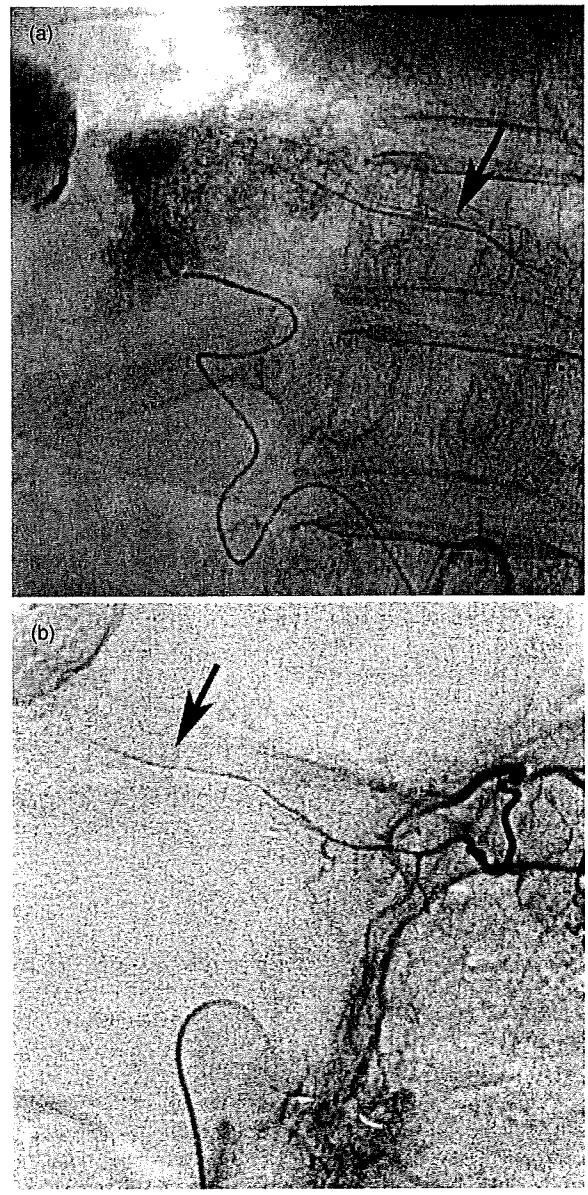

Fig. 3. (a) Spot radiograph during transcatheter arterial chemoembolisation of a small tumour-feeding branch of the medial segmental artery of the liver shows retrograde opacification of a small branch (arrow). (b) Arteriogram of the left inferior phrenic artery obtained after chemoembolisation shows the branch of the left inferior phrenic artery with inflow of embolic material (arrow).

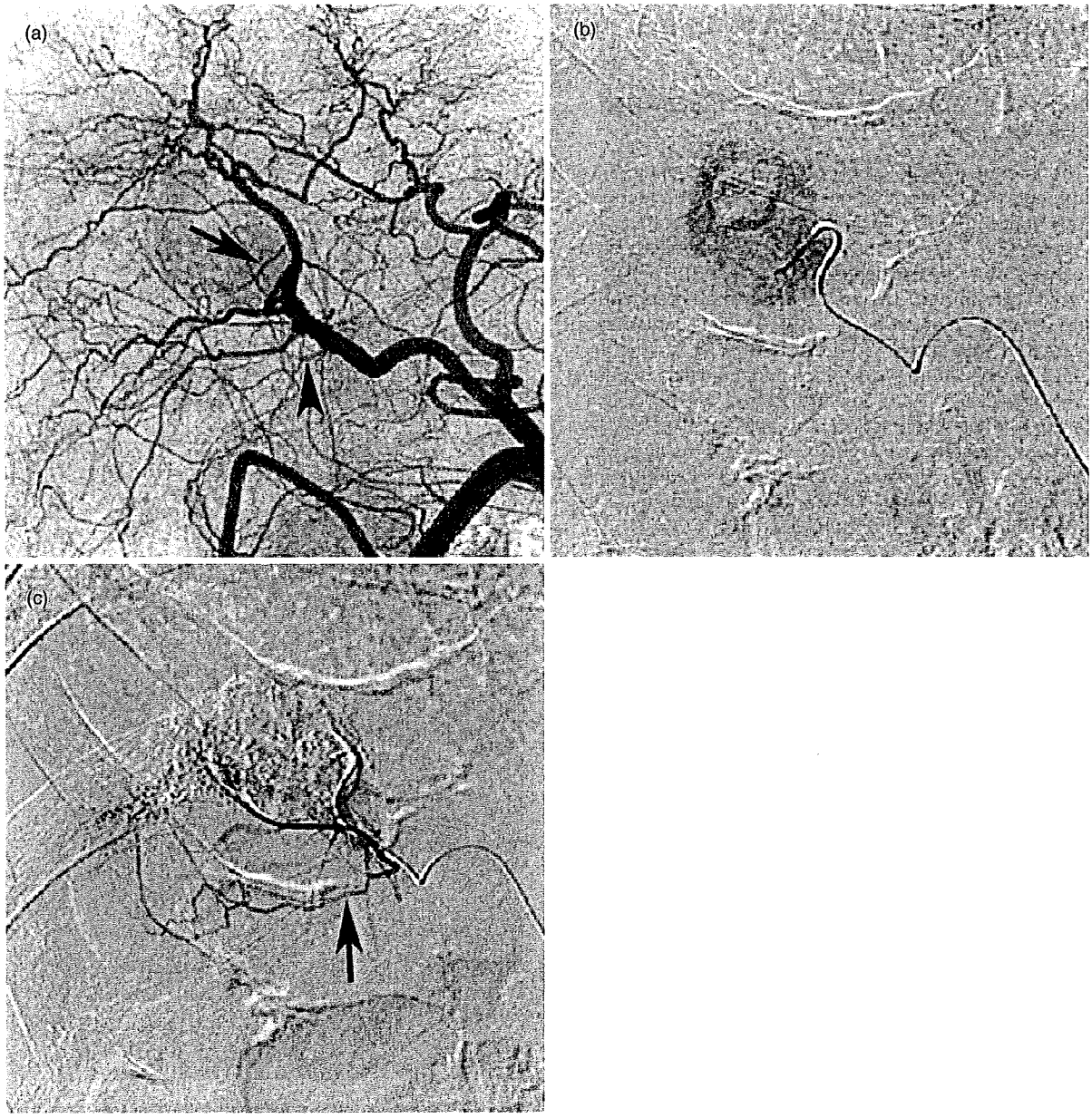

Fig. 4. (a) Arteriogram of the common hepatic artery shows a tumour stain supplied by a small branch of the anterior inferior subsegmental artery of the right hepatic artery (arrow). The arrowhead indicates the cystic artery. (b) The feeding branch was selected, and transcatheter arterial chemoembolisation was carried out. (c) Arteriogram of the feeding branch obtained after chemoembolisation shows the cystic artery through anastomosis (arrow).

Anastomosis between hepatic and extrahepatic vessels

Between the hepatic artery and the inferior phrenic artery

The inferior phrenic artery (IPA) is infrequently shown through the hepatic arterial branch. In our experience, the right IPA was shown through the caudate arterial branch (Fig. 1) and through the medial segmental artery derived from the left hepatic artery (Fig. 2). The left IPA was shown through the medial segmental artery derived from the left hepatic artery (Fig. 3), and dorsal lateral subsegmental artery of the left hepatic artery. It is usually shown during the injection of embolic material at the distal level of the hepatic artery. The IPA ascends along the diaphragmatic crura and supplies the liver through anastomoses at the bare area of the liver within the triangular ligaments, and anastomoses with the posterior intercostal artery (ICA) and musculophrenic artery of the internal mammary artery (IMA).[13]

Between the hepatic artery and the cystic artery

The cystic artery is infrequently shown on arteriogram of the hepatic branch distributing to the gall bladder bed. In our experience, this anastomosis was shown on arteriogram of the anterior inferior subsegmental artery of the right hepatic artery (Fig. 4) and medial segmental artery of the left hepatic artery (Fig. 5). We also saw the right hepatic artery on arteriogram of the cystic artery arising from the superior mesenteric artery. Generally, a deep branch of the cystic artery connects with the anterior branch of the right hepatic artery. In addition, part of the anterior inferior subsegmental branches from the cystic artery directly penetrates the liver through the gall bladder fossa.[14] Similarly, the connection between the medial segmental artery and the cystic artery may also be present. These anastomoses may cause tumour recurrence located near the gall bladder bed and gall bladder infarction after TACE despite avoiding cystic artery embolisation. Conversely, this anastomosis may also salvage gall bladder ischaemia acting as collateral circulation when the cystic artery is inadvertently embolised.

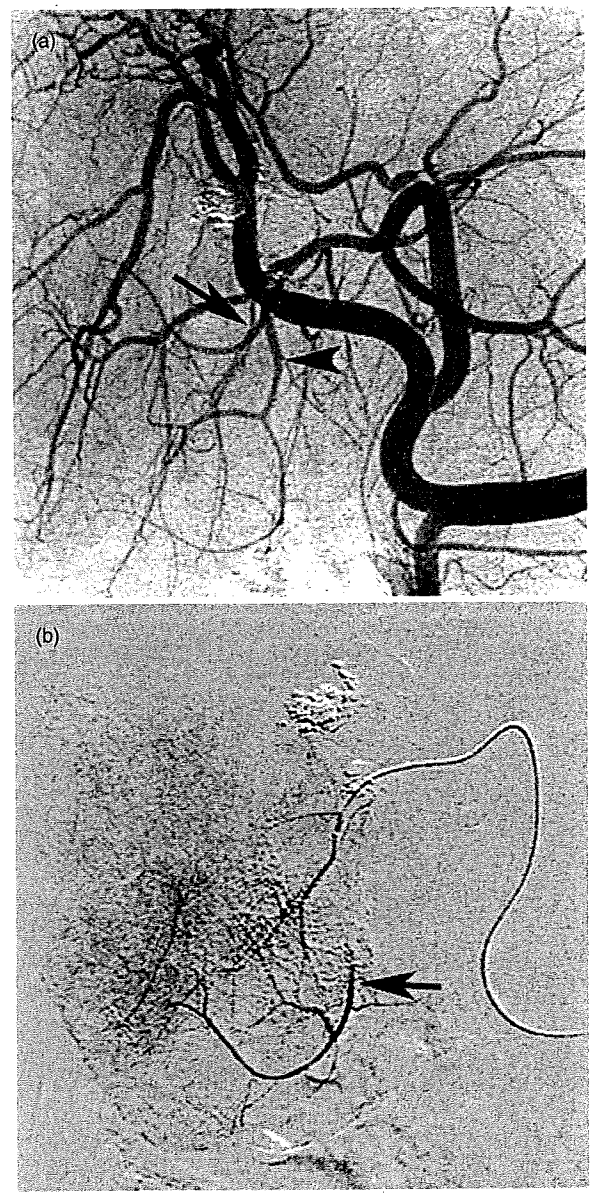

Fig. 5. (a) The arrow indicates a small branch of the medial segmental artery of the liver, and the arrowhead indicates the cystic artery. (b) Arteriogram of a small branch on (a) shows the cystic artery through anastomosis (arrow).

Between the caudate arterial branch o f the liver and the right renal capsular artery (RCA)

The caudate arterial branch of the liver is infrequently shown on arteriogram of the right RCA (Fig. 6). The right RCA feeds a tumour mainly located near the right renal fossa,[1,2,5] in addition to a tumour in the caudate lobe. The anastomoses between the caudate arterial branch and retroperitoneal arteries within the bare area of the liver may be potentially present and may make endovascular management of a tumour in the caudate lobe difficult.

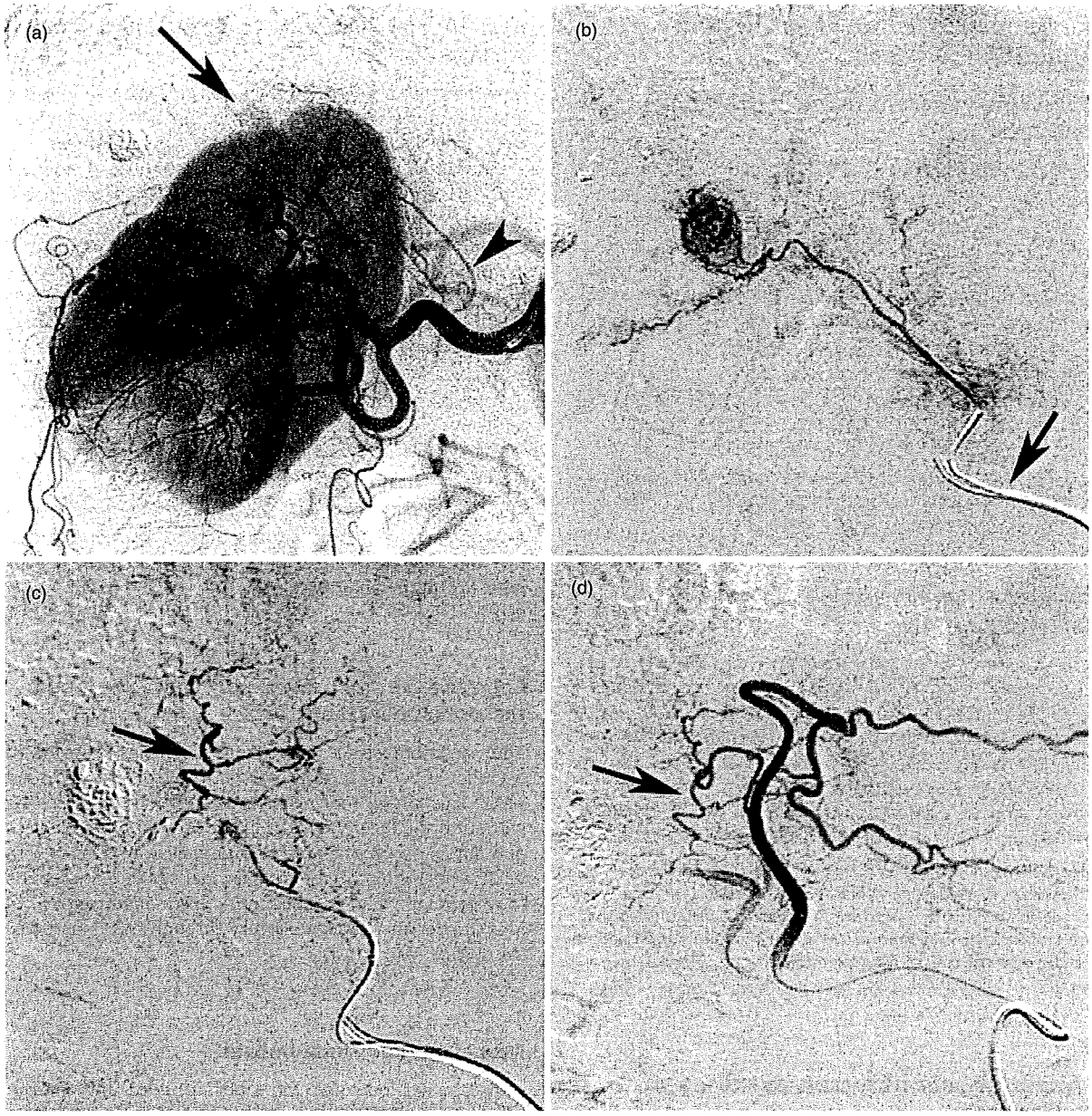

Fig. 6. (a) Arteriogram of the right renal artery shows a tumour stain (arrow) supplied by the right renal capsular artery (arrowhead). (b) The right renal capsular artery was selected, and transcatheter arterial chemoembolisation was carried out. The microcatheter was advanced into the right renal capsular artery through a side hole of a 4-F catheter (arrow). (c) Arteriogram obtained after chemoembolisation of the right renal capsular artery shows a small vessel that is not seen on (b). (d) Arteriogram of the left hepatic artery shows that the vessel is the caudate arterial branch of the liver (arrow).

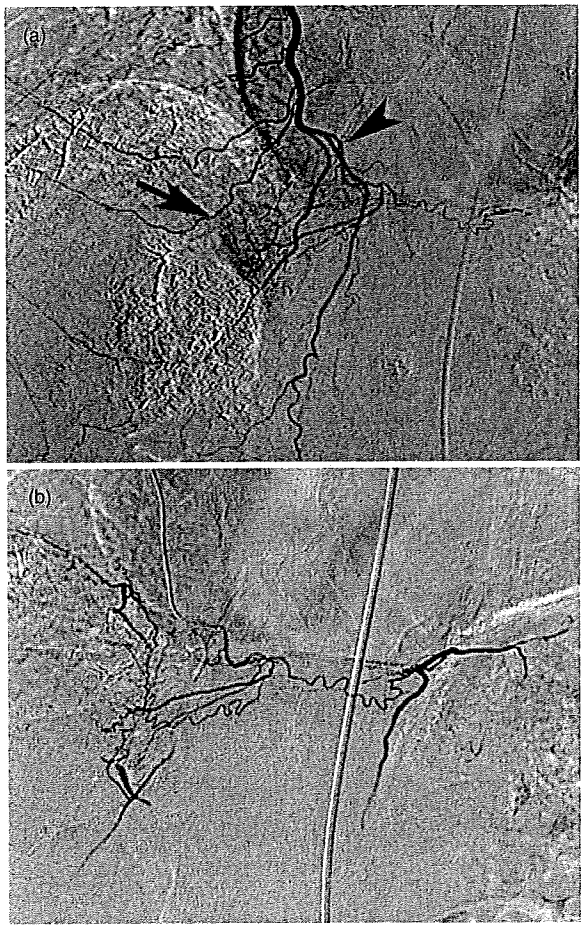

Fig. 7. (a) Arteriogram of the right internal mammary artery shows a tumour stain (arrow) supplied by a small branch of the musculophrenic artery (arrowhead). (b) The feeding branch was selected, and transcatheter arterial chemoembolisation was carried out. Arteriogram obtained after chemoembolisation shows the bilateral inferior phrenic arteries through the anastomosis.

Anastomosis between extrahepatic collaterals

Between the IMA and the IPA

This anastomosis is anatomically well known, but there have been no imaging reports. The musculophrenic artery of the IMA anastomoses with the IPA within the triangular ligaments (Fig. 7).[13] This anastomosis may explain the fact that a tumour located at the dome of the right lobe of the liver is frequently supplied by both arteries synchronously or asynchronously.[2] Some branches of the superior epigastric artery of the IMA extend into the falciform ligament of the liver and anastomose with the left hepatic artery.[10]

Between the posterior ICA or lumbar artery and the IPA

Anastomosis between the posterior ICA or lumbar artery and the IPA, in addition to the IMA, is anatomically well known; however, it is seldom shown on angiography (Figs 8,9). Lower posterior ICAs anastomose with the lateral branches of the IPA at the insertion site of the diaphragm on the lateral and posterior thoracic walls, and terminal branches of the upper lumbar arteries may also anastomose with branches from the lower ICAs.[6] Inflow of embolic material from the IPA to the posterior ICA may cause skin necrosis and spinal infarction.[6]

Between the right posterior ICA and the right RCA

This anastomosis is part of the retroperitoneal fine network acting as a collateral pathway to the occluded IPA[7] and may be present within the bare area of the liver near the right renal fossa (Fig. 10).

Between the right middle adrenal artery and the dorsal pancreatic artery

This anastomosis is frequently seen in cases with occluded IPA, as a collateral pathway of the occluded IPA.[7] This anastomosis is also rarely shown in cases without occluded IPA (Fig. 11). Several adrenal arteries and dorsal pancreatic artery potentially anastomose with each other within the retroperitoneal space. Pancreatitis may develop when embolic materials inadvertently flow into the dorsal pancreatic artery through this anastomosis during TACE.

Miscellaneous anastomoses

Anastomoses between the right superior and inferior adrenal arteries, between the several omental arteries or between the omental artery and the right colic artery (Fig. 12), and between the serial posterior ICAs or lumbar arteries are also observed. These connections are shown in many cases during TACE of these vessels. Anastomosis between omental artery and colic artery may cause colonic ischaemia after TACE.

Conclusions

Recognition of anastomosis between the hepatic artery and the extrahepatic collateral or between extrahepatic

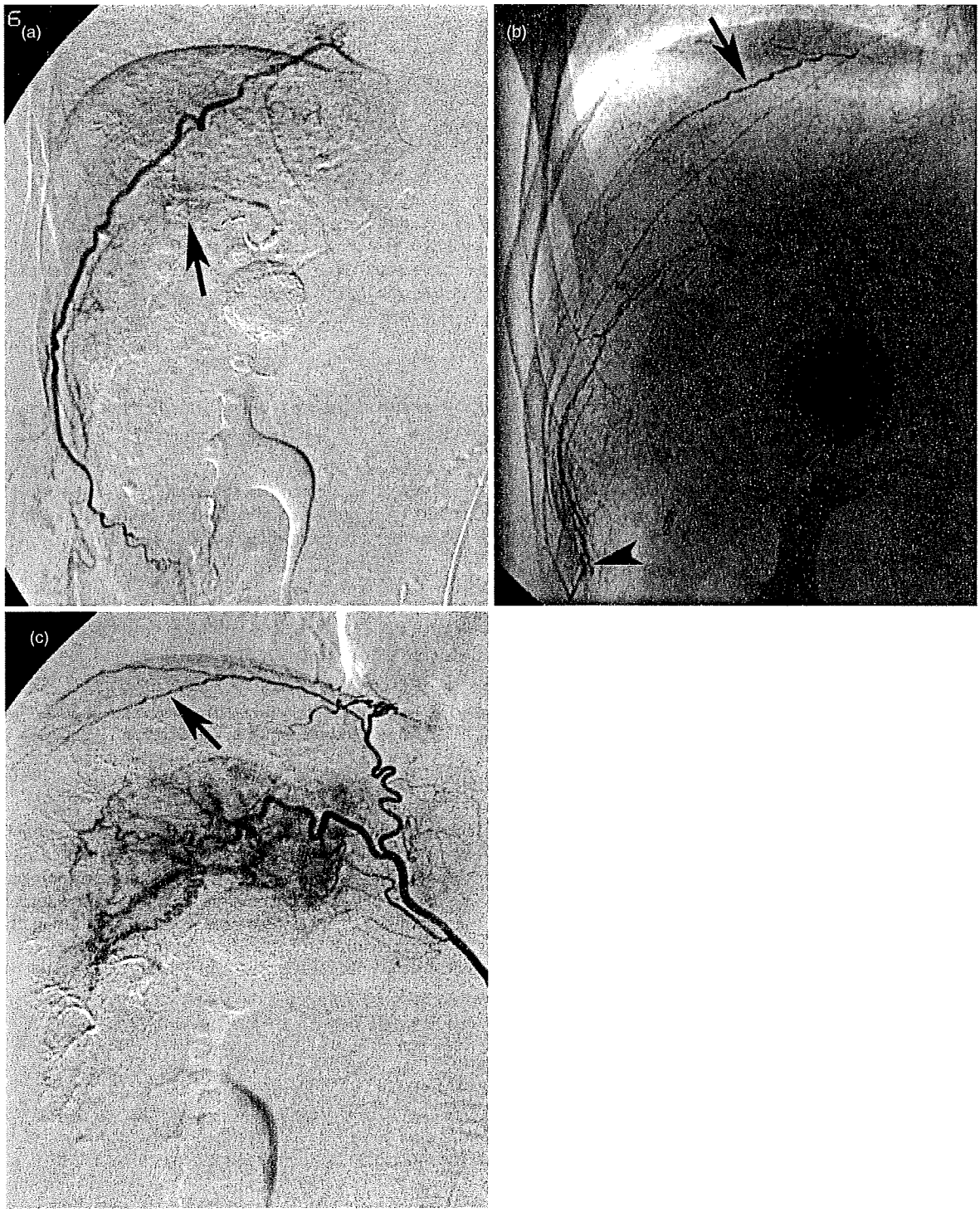

Fig. 8. (a) Arteriogram of the right 10th posterior intercostal artery shows a faint tumour stain (arrow). (b) The microcatheter was advanced across the costochondral junction, and transcatheter arterial chemoembolisation was carried out. Spot radiograph obtained during chemoembolisation shows a branch filled with iodised oil (arrow). The arrowhead indicates the catheter tip. (c) Arteriogram of the right inferior phrenic artery obtained before chemoembolisation of the right 10th posterior intercostal artery shows the branch seen in (b) (arrow).

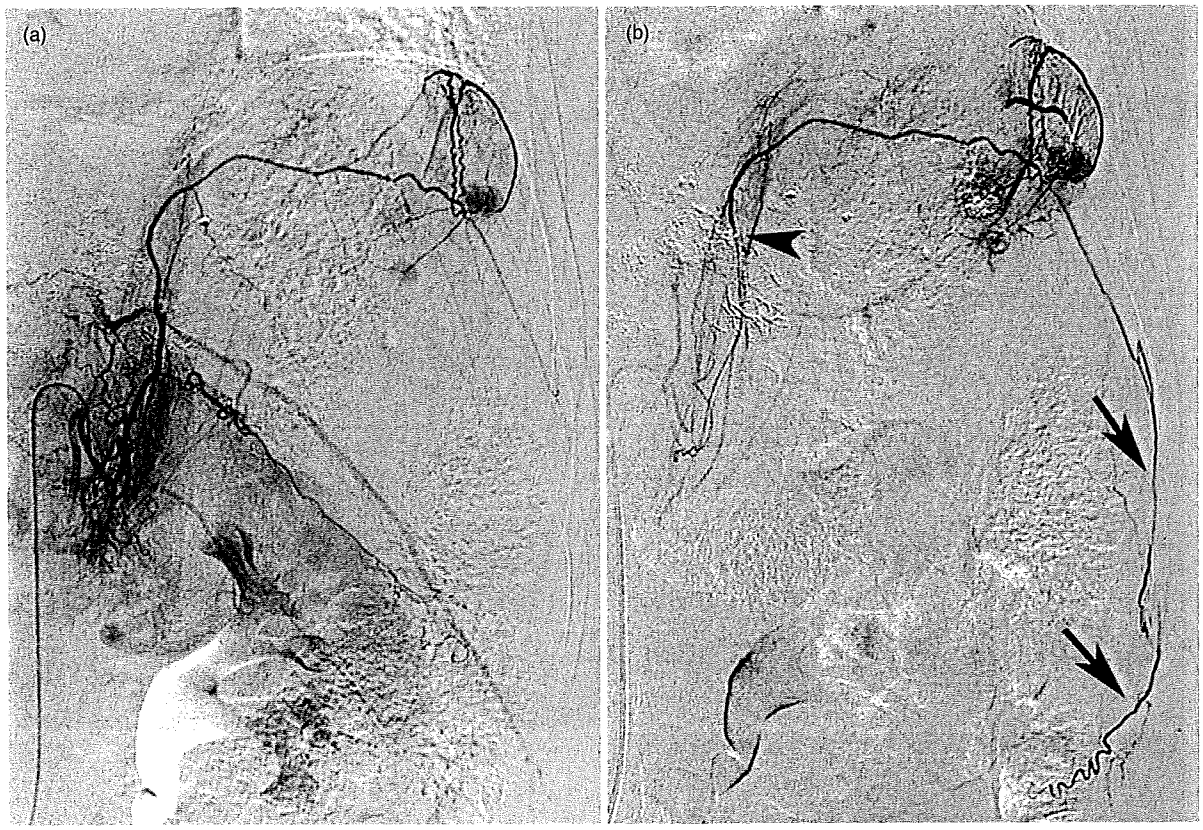

Fig. 9. (a) Arteriogram of the left inferior phrenic artery shows multiple tumour stains. (b) Arteriogram of the left inferior phrenic artery after distal advancement of the microcatheter shows two left posterior intercostal arteries through the anastomoses (arrows). Arrowhead indicates microcatheter tip.

collaterals is important to complete an effective TACE procedure. These anastomoses may be potentially present in almost all cases although angiography rarely shows these anastomoses because the anastomosing branches are too small. Arterial blood through these anastmoses may promote survival of tumour tissue or cause tumour recurrence after TACE. On the other hand, some embolic materials injected with slight force pass through these anastomoses, and unexpected complications may develop. Radiologists should pay considerable attention to these anastomoses, especially during the TACE procedure.

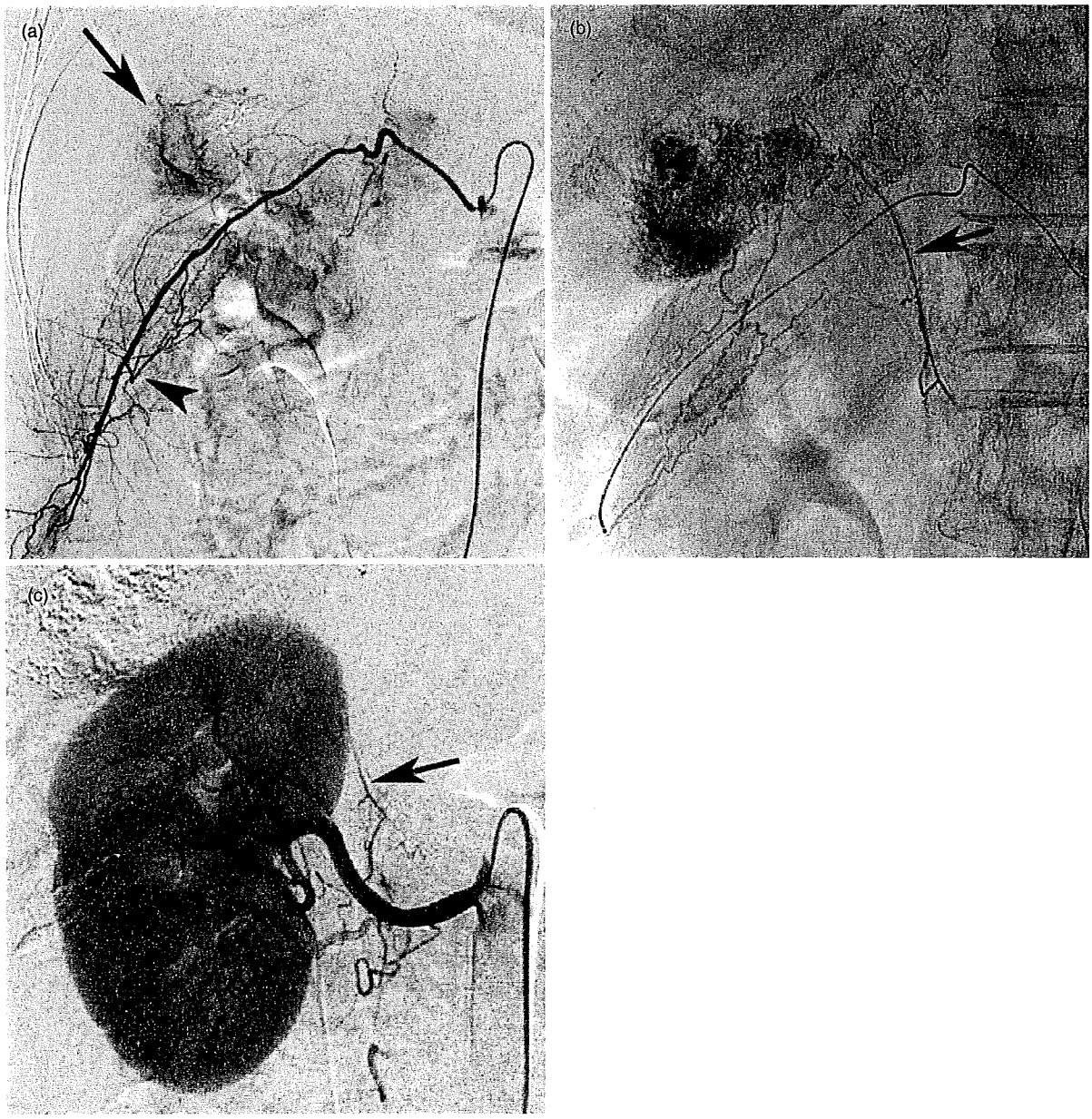

Fig. 10. (a) Arteriogram of the right 11th posterior intercostal artery shows a tumour stain (arrow) supplied by a small feeding branch (arrowhead). (b) The feeding branch was selected, and transcatheter arterial chemoembolisation was carried out. A small vessel is shown during chemoembolisation that is not seen on (a) (arrow). (c) Arteriogram of the right renal artery shows the right renal capsular artery with inflow of embolic material (arrow).

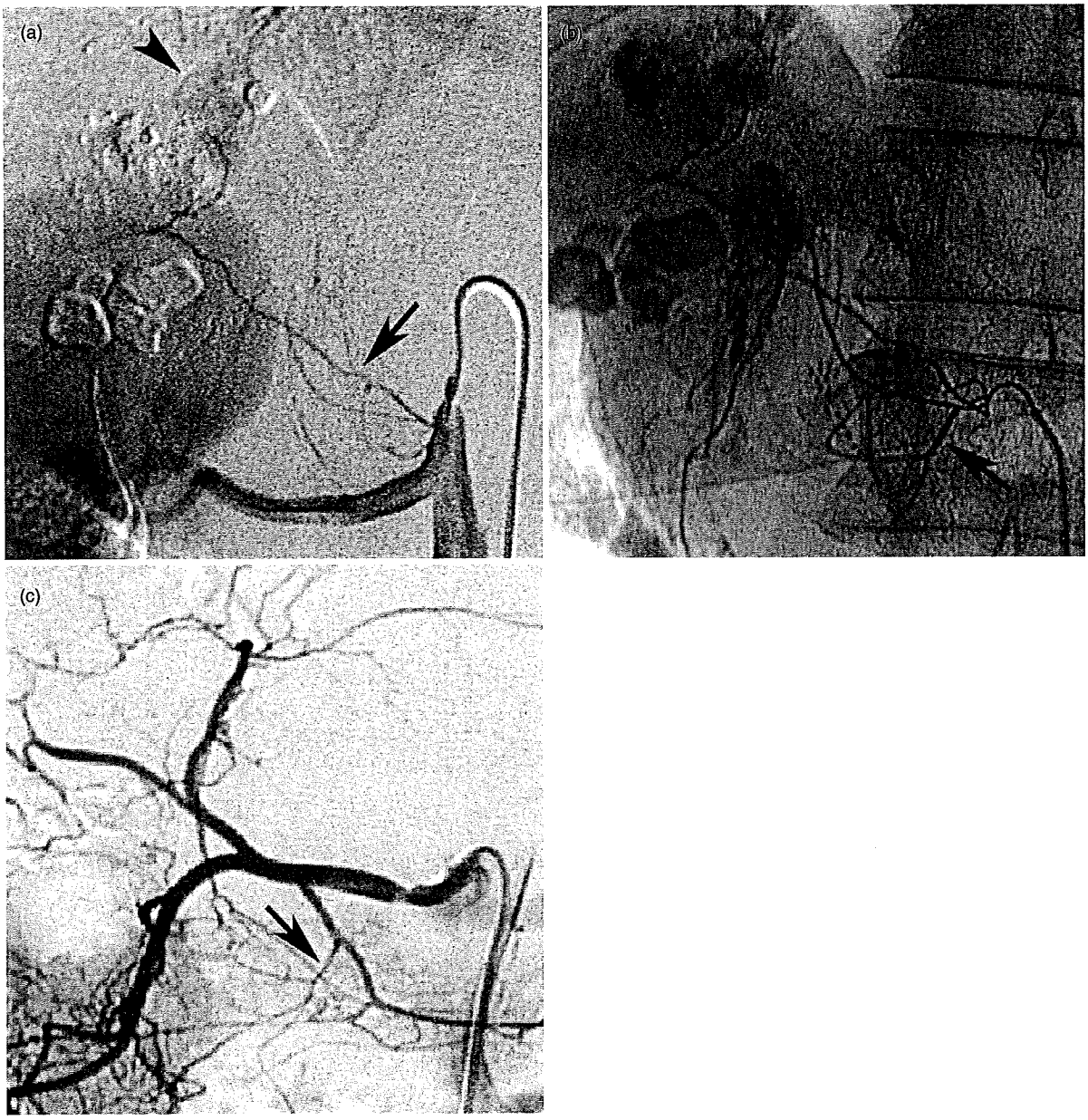

Fig. 11. (a) Arteriogram shows that a tumour (arrowhead) is fed by the right middle adrenal artery arising from the aorta (arrow). (b) Spot radiograph obtained during transcatheter chemoembolisation shows a vessel that is not seen in (a) (arrow). (c) Arteriogram of the common hepatic artery reveals that the vessel is the dorsal pancreatic artery derived from the common hepatic artery (arrow).

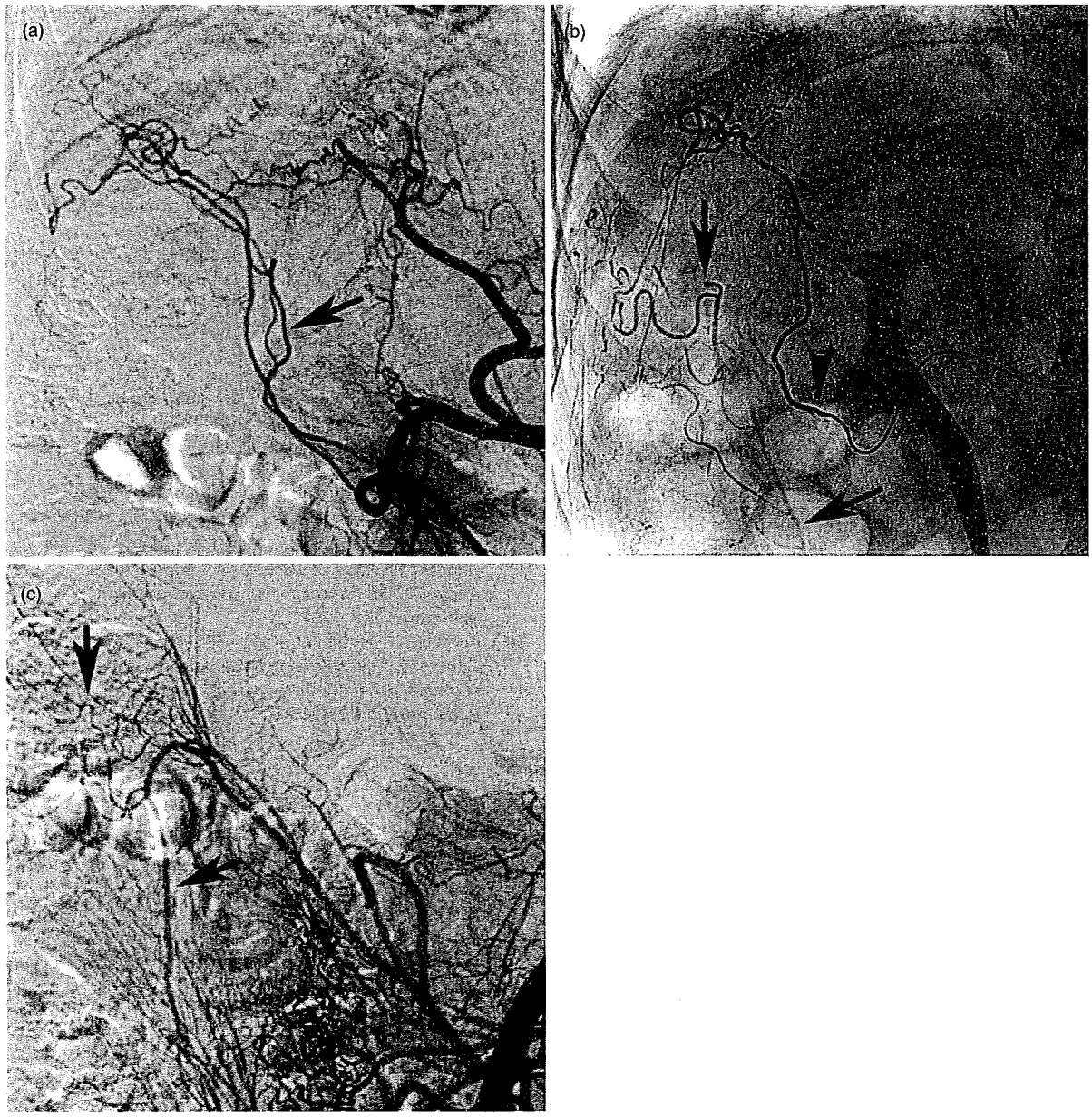

Fig. 12. (a) Coeliac arteriogram shows two hypertrophied omental arteries supplying tumour (not shown). One omental artery was selected, and transcatheter arterial chemoembolisation was carried out (arrow). (b) Spot radiograph obtained during chemoembolisation shows retrograde opacification of a vessel that is not seen in (a) (arrows). The arrowhead indicates the microcatheter tip. (c) Arteriogram of the superior mesenteric artery reveals that the vessel is the right colic artery (arrows).

References

1. Kim HC, Chung JW, Lee W *et al.* Recognizing extrahepatic collateral vessel that supply hepatocellular carcinoma to avoid complications of transcathether arterial chemoembolization. *Radiographics* 2005; **25**: S25–S39.
2. Miyayama S, Matsui O, Taki K *et al.* Extrahepatic blood supply to hepatocellular carcinoma: angiographic demonstration and transcatheter arterial chemoembolization. *Cardiovasc Intervent Radiol* 2006; **29**: 3–48.
3. Chung JW, Park JH, Han JK, Choi BI, Kim TK, Han MC. Transctheter oily chemoembolization of the inferior phrenic artery in hepatocellular carcinoma: the safety and potential therapeutic role. *J Vasc Interv Radiol* 1998; **9**: 495–500.
4. Hirota S, Matsumoto S, Fukuda T, Yoshikawa T, Motohara T, Ichikawa S. Solitary hepatocellular carcinoma fed by the cystic artery: limitation of transcatheter arterial embolization. *Cardiovasc Intervent Radiol* 1999; **22**: 206–9.
5. Kodama Y, Shimizu T, Endo H *et al.* Spontaneous rupture of hepatocellular carcinoma supplied by the right renal capsular artery treated by transcatheter arterial embolization. *Cardiovasc Intervent Radiol* 2002; **25**: 137–40.
6. Park SI, Lee Y, Won JY, Lee TJ. Extrahepatic collateral supply to hepatocellular carcinoma fed by the intercostal arteries. *J Vasc Interv Radiol* 2003; **14**: 461–8.
7. Miyayama S, Matsui O, Taki K *et al.* Transcatheter arterial chemoembolization for hepatocellular carcinoma fed by the reconstructed inferior phrenic artery: anatomical and technical analysis. *J Vasc Interv Radiol* 2004; **15**: 815–23.
8. Miyayama S, Matsui O, Nishida H *et al.* Transcatheter arterial cheoembolization for unesectable hepatocellular carcinoma fed by the cystic artery. *J Vasc Interv Radiol* 2003; **14**: 1155–61.
9. Nakai M, Sato M, Kawai N *et al.* Hepatocellular carcinoma: involvement of the internal mammary artery. *Radiology* 2001; **219**: 147–52.
10. Kim HC, Chung JW, Choi SH, Jae HJ, Lee W, Park JH. Internal mammary arteries supplying hepatocellular carcinoma: vascular anatomy at digital subtraction angiography in 97 patients. *Radiology* 2007; **242**: 925–32.
11. Miyayama S, Matsui O, Akakura Y *et al.* Hepatocellular carcinoma with blood supply from omental branches: treatment with transcatheter arterial embolization. *J Vasc Interv Radiol* 2001; **12**: 1285–90.
12. Charnsangavej C, Chuang VP, Wallace S, Soo CS, Bowers T. Angiographic classification of hepatic arterial collaterals. *Radiology* 1982; **144**: 485–94.
13. Uflacker R. *Atlas of Vascular Anatomy: An Angiographic Approach*. Williams and Wilkins, Baltimore, MD, 1997.
14. Komatsu T, Matsui O, Kadoya M, Yoshikawa J, Gabata T, Takashima T. Cystic artery origin of the segment V hepatic artery. *Cardiovasc Intervent Radiol* 1999; **22**: 165–7.

Cardiovasc Intervent Radiol
DOI 10.1007/s00270-009-9638-z

CASE REPORT

Sloughing of Intraductal Tumor Thrombus of Hepatocellular Carcinoma After Transcatheter Arterial Chemoembolization

Miho Okuda · Shiro Miyayama · Masashi Yamashiro · Yuichi Yoshie · Natsuki Sugimori · Saya Igarashi · Yoshiko Nakashima · Taku Sanada · Shotaro Kosaka · Daishu Toya · Osamu Matsui

Received: 30 March 2009 / Accepted: 2 June 2009

Abstract Transcatheter arterial chemoembolization (TACE) is effective for hepatocellular carcinoma (HCC) with intrabile duct thrombus. After TACE, intraductal tumor thrombi occasionally detach from the intrahepatic tumor and drop into the bottom of the common bile duct, causing clinical symptoms similar to the impaction of choledocholithiasis. The investigators describe three cases of sloughing of HCC intraductal tumor thrombi after selective TACE. In each of the three cases, the necrotic tumor cast was successfully removed endoscopically, and the patient's symptoms were dramatically improved. Two patients survived without recurrence of the intraductal tumor thrombus for 8 and 11 months after TACE, respectively.

Keywords Hepatocellular carcinoma · Intraductal tumor thrombus · Transcatheter arterial chemoembolization · Sloughing of tumor thrombus

M. Okuda (✉) · S. Miyayama · M. Yamashiro · Y. Yoshie · N. Sugimori · S. Igarashi · Y. Nakashima
Department of Radiology, Fukuiken Saiseikai Hospital, 7-1 Funabashi, Wadanaka-cho, Fukui 918-8503, Japan
e-mail: kusanagi_miho@mbr.nifty.com

T. Sanada · S. Kosaka · D. Toya
Department of Internal Medicine, Fukuiken Saiseikai Hospital, 7-1 Funabashi, Wadanaka-cho, Fukui 918-8503, Japan

O. Matsui
Department of Radiology, Kanazawa University Graduate School of Medical Science, 13-1 Takaramachi, Kanazawa 920-8641, Japan

Published online: 16 July 2009

Introduction

Although invasion into the portal vein is a common feature in hepatocellular carcinoma (HCC), intraductal tumor thrombus is considered to be rare [1, 2]. Transcatheter arterial chemoembolization (TACE) is one of the most effective therapeutic options for unresectable HCC, and it is also accepted procedure for tumor thrombi in the bile duct [3]. In this report, we describe three patients presenting with biliary obstruction caused by sloughing of an HCC intraductal tumor thrombus after TACE.

Case Reports

Case No. 1

A 61-year-old woman with HCC associated with liver cirrhosis secondary to hepatitis C and alcohol use was admitted to our hospital. She had previously undergone two TACE sessions for HCC in the past 30 months. Computed axial tomography (CAT) showed a recurrent tumor, 1.5 cm in diameter, with an intraductal tumor thrombus in segment IV and dilatation of the left bile duct system (Fig. 1A). She was not a suitable candidate for surgical resection because of her limited hepatic function. On admission, her serum bilirubin level was 3.2 mg/dl. It gradually increased to 7.4 mg/dl; however, it then spontaneously decreased to 3.1 mg/dl after 1 month. TACE was selectively performed in both hepatic arterial branches in segments IV and VIII without serious complications. Seven days after TACE, she presented with epigastric pain and fever. Her serum bilirubin level increased from 2.7 to 13.8 mg/dl. CAT showed dense iodized oil accumulation in the tumor and disappearance of the intraductal tumor thrombus (Fig. 1B). A

hyperattenuating mass was seen at the bottom of the common bile duct, and the entire biliary system was dilated (Fig. 1C). We decided that the necrotic tumor thrombus had detached from the main tumor and dropped into the common bile duct, causing biliary obstruction. Two days later, the necrotic thrombus was removed endoscopically (Fig. D). After removal of the necrotic tissue, she was free of symptoms, and her serum bilirubin level returned to normal. The tumor in segment IV recurred 5 months later and was successfully treated by additional TACE. There has been no recurrence of the intraductal tumor thrombus for 8 months.

Case No. 2

An 82-year-old woman with HCC associated with liver cirrhosis caused by unknown etiology was admitted because of abdominal pain and jaundice. She had previously been treated with three TACE sessions during the course of 22 months. CAT showed multiple HCC in both lobes of the liver. The main tumor was 1.8 cm in diameter and was located in the hepatic hilum; however, it had invaded into the right hepatic duct and caused dilatation of the biliary system (Fig. 2A). Magnetic resonance imaging (MRI) demonstrated blood degradation products in the common bile duct in addition to an intraductal tumor thrombus (Fig. 2B). Because of her poor hepatic function reserve, she was assessed as being inoperable. On admission, her serum bilirubin level was 9.1 mg/dl. It gradually increased to 16.1 mg/dl; however, it then spontaneously decreased to 2.8 mg/dl after 1 month. TACE was selectively performed through the right hepatic arterial branches without serious complications. CAT obtained 7 days after TACE showed dense iodized oil accumulation in the main tumor and intraductal tumor thrombus. The intraductal tumor thrombus had shrunk slightly and migrated distally (Fig. 2C). Ten days after TACE, she presented with epigastric pain, fever, and jaundice. Her serum bilirubin level increased from 2.3 to 4.5 mg/dl. Sloughing of the intraductal thrombus into the bottom of the common duct and dilatation of the bile duct were confirmed on CAT (Figs. 2D and 2E). The necrotic tissue was removed endoscopically, and her symptoms improved. During the 11 month follow-up period, local recurrent tumors and newly developed tumors at other sites were treated by two additional TACE sessions. The bile duct tumor thrombus has not recurred for 15 months.

Case No. 3

A 71-old-woman with HCC associated with liver cirrhosis secondary to hepatitis C was admitted. She had undergone

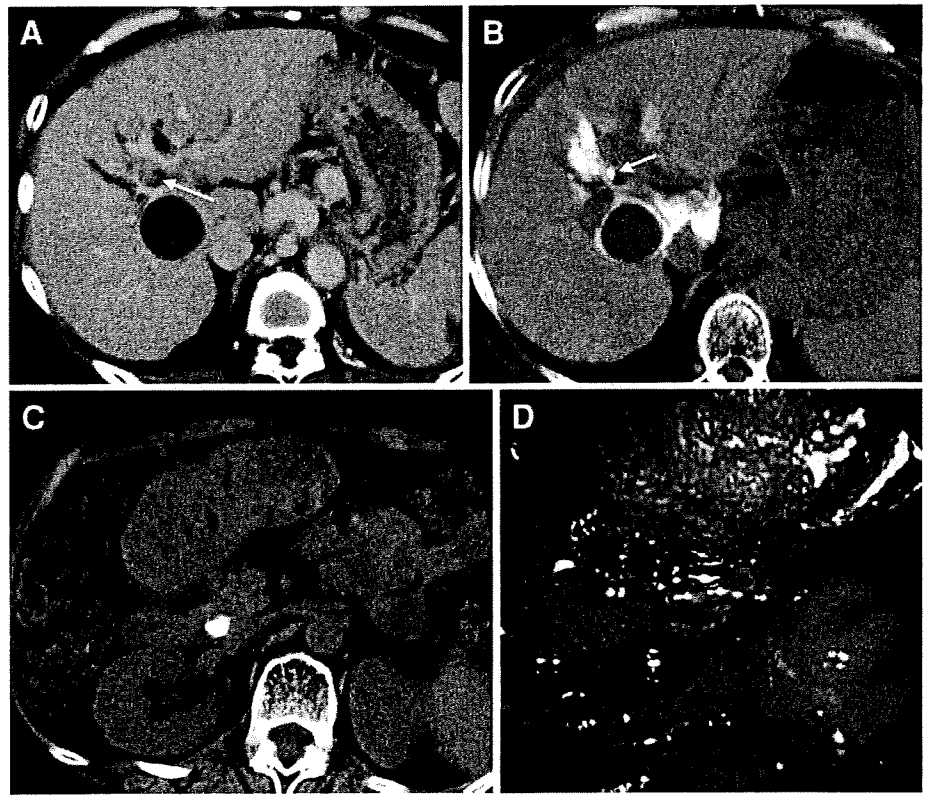

Fig. 1 Case no. 1. **A** Contrast-enhanced CAT image before TACE shows a recurrent tumor with an intraductal tumor thrombus (*arrow*) in segment IV and dilatation of the left bile duct system. **B** Unenhanced CAT 7 days after TACE shows dense iodized oil accumulation in the hepatic tumor and disappearance of the intraductal tumor thrombus (*arrow*). **C** On the CAT image at the bottom of (**B**), a hyperattenuating mass is seen at the bottom of the common bile duct, indicating a sloughed tumor with iodized oil accumulation. **D** The necrotic tissue was endoscopically removed, and the patient's symptoms improved dramatically

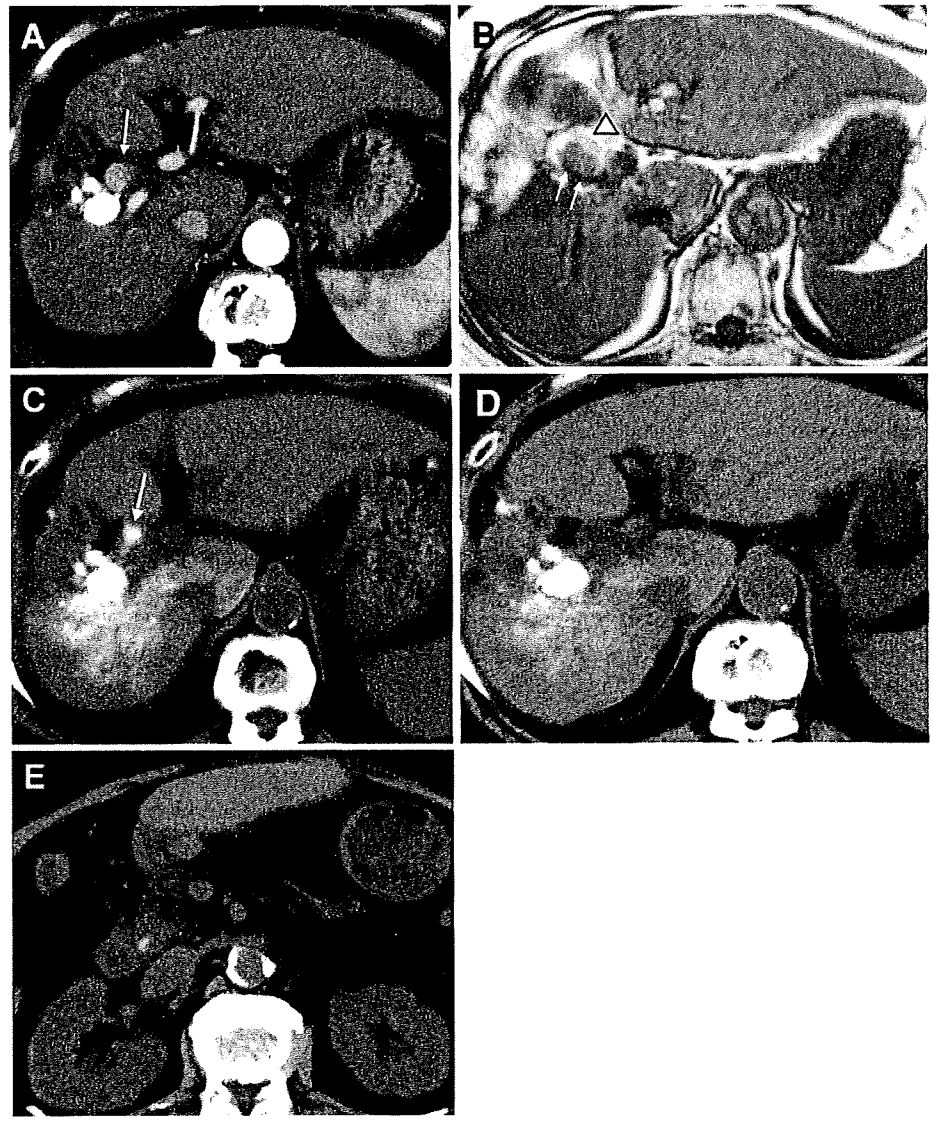

Fig. 2 Case no. 2. **A** Arterial-phase CAT shows an intraductal tumor thrombus in the right hepatic duct (*arrow*). **B** Axial T1-weighted MRI demonstrates the intraductal tumor (*arrows*) and hemobilia (*arrowhead*). **C** Unenhanced CAT 7 days after TACE shows dense iodized oil accumulation in the tumor and intraductal tumor thrombus (*arrow*). The tumor thrombus has shrunk slightly and migrated distally. **D** Unenhanced CAT 10 days after TACE shows the disappearance of the intraductal tumor thrombus. **E** At the bottom of the CAT image shown in (**D**), the tumor thrombus has sloughed into the common bile duct

seven TACE sessions for HCC during the course of 3 years. CAT showed multiple HCC in both lobes of the liver and tumor thrombi in the right hepatic and common bile ducts. She was not a suitable candidate for surgical resection because of her poor general condition. TACE was performed through the right hepatic artery without serious complications. Seven days after TACE, she presented with epigastric pain, and sloughing of the intraductal tumor thrombus and dilatation of the bile duct were confirmed on CAT. Her serum bilirubin level increased from 2.6 to 15.3 mg/dl. The necrotic tissue was removed endoscopically, and her symptoms improved. Her serum bilirubin level decreased after removal of the detached tumor thrombus; however, she died of intrahepatic tumor progression 38 days after TACE.

Discussion

HCC with intrabile duct invasion is less common than invasion into the portal vein. Intraductal tumor thrombi cause hemobilia and/or jaundice and rapid deterioration of hepatic function. Lin [1] classified such cases as "icteric hepatoma." Kojiro et al. [2] described the features of 24 cases of HCC with prominent intrabile duct tumor growth among 238 autopsy and 21 surgical cases, with a prevalence of approximately 9%. In their series, the survival time of patients with intraductal tumor growth was significantly shorter than that of patients without bile duct invasion in their series [2]. In contrast, it has also been reported that not all patients with HCC intrabile duct invasion are terminally ill, and good

palliation and occasional cure may be possible with proper management [4].

The ideal treatment for patients with intraductal tumor thrombus is surgical resection [5, 6]. However, most tumors with bile duct invasion are generally large and located near the hepatic hilum. Such patients usually have poor hepatic function reserve; therefore, most patients are not candidates for surgery. Kitagawa et al. [3] reported the efficacy of TACE for controlling hemobilia caused by advanced HCC rupturing into the biliary system. In their series, hemobilia was temporarily stopped by TACE in all three patients. They stated that selective TACE was safe and effective for managing hemobilia in the selected patients with even far-advanced HCC.

Hiraki et al. [7] reported a case of sloughing of intraductal tumor thrombus who presented with jaundice and severe back pain 18 days after TACE. The clinical symptoms were improved after endoscopic removal of the tumor cast in the bile duct. Tumor thrombi in the bile duct are usually histologically similar to the main tumor; however, they generally become more necrotic and hemorrhagic. In addition, tumors growing into the bile duct usually do not attach tightly to the bile duct wall [2]. In a report by Yamamoto et al. [8], an intraductal tumor thrombus was removed by endoscopic catheter insertion alone. In our three cases, as in a case reported by Hiraki et al. [7], the bile duct tumor thrombus was easily detached and dropped into the common bile duct after TACE. This suggests that TACE has a strong therapeutic effect and achieves complete necrosis of the intraductal tumor thrombus. Therefore, physicians should recognize the risk of obstructive jaundice and acute pancreatitis caused by sloughing of the intraductal tumor thrombus after TACE [7].

The clinical symptoms and management of dropped intraductal tumors are similar to those of the impaction of choledocholithiasis. In our three cases, the necrotic tumor cast was successfully removed endoscopically. We believe that endoscopic removal is the most desirable and effective treatment. To remove the necrotic tissue, however, endoscopic sphincterectomy (EST) may be necessary. Most patients with liver cirrhosis have hypersplenism-related thrombocytopenia; therefore, platelet transfusion may frequently be required to perform EST. Endoscopic tube stent insertion into the common bile duct may also be useful to relieve jaundice in patients with poor general condition. There have not been enough reports discussing the usefulness of prophylactic biliary drainage in such patients. We believe endoscopic intervention should be considered when a symptomatic sloughed tumor develops because not all intraductal tumor thrombi may drop after TACE.

In the present two cases (case nos. 1 and 2), a relatively small tumor located near the hepatic hilum progressed into the bile duct. In such cases, TACE may provide sufficient effects not only on the main tumor but also against the intraductal tumor thrombus. In our two patients, the intraductal tumor thrombus disappeared and has not recurred for > 8 and 11 months, respectively. In addition, the recurrent tumor and newly developed tumors were well controlled by TACE in both patients. Therefore, we conclude that intraductal tumor thrombus may not be a terminal illness and rather can be successfully managed by selective TACE in certain patients, especially when the main tumor is relatively small.

TACE is generally contraindicated for patients with hyperbilirubinemia. Okazaki et al. [9] performed TACE in 38 patients with intraperitoneal hemorrhage secondary to HCC, and there was a significant difference in the survival period between 24 patients without hyperbilirubinemia and 14 patients with hyperbilirubinemia > 3 mg/dl. Considering hepatic function, it is preferable that TACE is performed in patients with a low bilirubin level. Although in the present two cases (case nos. 1 and 2), the patients' bilirubin levels were high on admission, they decreased to approximately 3 mg/dl after 1 month of medical therapy; therefore, we were able to perform effective TACE without severe complications. However, we would not hesitate to perform TACE even in patients with hyperbilirubinemia when uncontrolled massive hemobilia from an intraductal tumor occurs [6]. In such conditions, the embolized arterial branches should be minimized so as not to deteriorate hepatic function further.

There is a limitation to the present study. Histopatologic confirmation of the dropped tumor thrombus was not obtained in all three cases because the mass was released into the duodenum after removal from the common bile duct. However, we believe that the removed mass was a completely necrotic intraductal tumor thrombus on the basis of serial CAT findings.

In conclusion, intraductal tumor thrombi may easily drop into the common bile duct after TACE and cause obstructive jaundice and acute pancreatitis, symptoms similar to choledocholithiasis. An endoscopic procedure may be required if clinical symptoms develop. TACE is effective for treating intraductal tumor thrombi and achieves sufficient results, especially if the main tumor is relatively small.

References

1. Lin TY (1976) Tumors of the liver. In: Bockus HL (ed) Gastroenterology. WB Saunders, Philadelphia, pp 522–533
2. Kojiro M, Kawabata K, Kawano Y, Shirai F, Takemoto N, Nakashima T (1982) Hepatocellular carcinoma presenting as intrabile duct tumor growth: a clinicopathologic study of 24 cases. Cancer 49:2144–2147

3. Kitagawa K, Yamakado K, Nakatsuka A, Tanaka N, Fujii A, Takano K et al (1999) Selective transcatheter hepatic arterial chemoembolization for hemobilia from hepatocellular carcinoma: report of three cases. J Vasc Interv Radiol 10:1357–1360
4. Chen MF, Jan YY, Jeng LB, Hwang TL, Wang CS, Chen SC (1994) Obstructive jaundice secondary to ruptured hepatocellular carcinoma into the common bile duct. Surgical experiences of 20 cases. Cancer 73:1335–1340
5. Lau WY, Leung JW, Li AK (1990) Management of hepatocellular carcinoma presenting as obstructive jaundice. Am J Surg 160:280–282
6. Tsuzuki T, Ogata Y, Iida S, Kasajima M, Takahashi S (1979) Hepatoma with obstructive jaundice due to the migration of a tumor mass in the biliary tract: report of a successful resection. Surgery 85:593–598
7. Hiraki T, Sakurai J, Gobara H, Kawamoto H, Mukai T, Hase S et al (2006) Sloughing of intraductal tumor thrombus of hepatocellular carcinoma after transcatheter chemoembolization causing obstructive jaundice and acute pancreatitis. J Vasc Interv Radiol 17:583–585
8. Yamamoto T, Sakamoto M, Ozawa T, Watanabe H, Nishida H, Mitamura K (2001) A case of hepatocellular carcinoma complicated with bile duct tumor thrombus removed by endoscopic catheter insertion after treatment of portal venous tumor thrombus [in Japanese]. Liver Cancer 1:99–104
9. Okazaki M, Higashihara H, Koganemaru F, Nakamura T, Kitsuki H, Hoashi T et al (1991) Intraperitoneal hemorrhage from hepatocellular carcinoma: emergency chemoembolization or embolization. Radiology 180:647–651